

SUPPLEMENTARY INFORMATION

1. Particle Characterization  
1.1. DOTAP liposome formulation

Supplementary Table 1.1: Formulation of DOTAP liposomes.

[DOTAP]	[DOPE-PEG1K]	Concentration (M)		Approximate [Liposome]
		[OG]	Total lipid	
$3.6 \times 10^{-4}$	$4.0 \times 10^{-5}$	$4.0 \times 10^{-6}$	$4.0 \times 10^{-4}$	$1 \times 10^{-9}$

1.2. DLS and ELS characterization  
See main text, Table 1.  
1.3. FS total charge calculations

Charge per FS particle was calculated using Equations 1.1 and 1.2, below.

$$P = \frac{6 \cdot C \cdot 10^{12}}{\rho \cdot \pi \cdot \phi^3} \quad \text{Eq. 1.1}$$

$$\text{Charge per particle} = \frac{C \cdot q}{P} \quad \text{Eq. 1.2}$$

Where  $P$  is number of particles per mL,  $C$  is concentration of suspended particles in g/mL (0.02 g/mL),  $\rho$  is the density of polystyrene (1.055 g/cm<sup>3</sup>),  $\phi$  represents the diameter of the FS in  $\mu\text{m}$ , and  $q$  is the charge density of the material, reported on the material certificate of analysis sheet (Supplementary Figure 1.1)

MOLECULAR PROBES®		CERTIFICATE OF ANALYSIS	
<b>Catalog Number</b>	F8801	<b>Catalog Number</b>	F8811
<b>Product Name</b>	FluoSpheres® carboxylate-modified microspheres, 0.1 $\mu\text{m}$ , red fluorescent (580/605) *2% solids*	<b>Product Name</b>	FluoSpheres® carboxylate-modified microspheres, 0.2 $\mu\text{m}$ , yellow-green fluorescent (505/515) *2% solids*
<b>Appearance</b>	pink suspension	<b>Appearance</b>	yellow suspension
<b>Medium</b>	distilled water, 2 mM sodium azide	<b>Medium</b>	distilled water, 2 mM azide
<b>Concentration</b>	$4.0 \times 10^{13}$ particles/mL	<b>Concentration</b>	$5.3 \times 10^{12}$ particles/mL
<b>Lot Number</b>	1985240	<b>Lot Number</b>	1927586
SONICATE WELL BEFORE USE. STORE AT 4°C, DO NOT FREEZE			
	LOT DATA	SPECIFICATION	
<b>FLUORESCENCE</b>			
Emission Maximum	606 nm		605 $\pm$ 5 nm
Relative Quantum Yield <sup>1</sup>	0.60		$\geq$ 0.40
<b>MICROSCOPY</b>			
Inspection	meets specification		few or no aggregates detectable after sonication
<b>TECHNICAL DATA<sup>2</sup></b>			
Actual Particle Size	$0.097 \pm 0.0080 \mu\text{m}$		n.a.
Charge	0.3559 meq/g		n.a.
Density of Polystyrene	1.055 g/cm <sup>3</sup>		n.a.
Specific Surface Area	$5.9 \times 10^5 \text{ cm}^2/\text{g}$		n.a.
<b>MISCELLANEOUS INFORMATION</b>			
Material Lot Number	1977342		n.a.
<ol style="list-style-type: none"> <li>Relative to a solution in chloroform of the dye used to prepare this product.</li> <li>Technical data for the unstained microspheres.</li> </ol>			
 Rachel Smith, Quality Assurance Manager 16-Mar-2018			
<small>Life Technologies Corporation, on behalf of its Invitrogen business, Molecular Probes® labeling and detection technologies, certifies on the date above that this is an accurate record of the analysis of the subject lot and that the data conform to the specifications in effect for this product at the time of analysis.</small>			
<small>Molecular Probes, Inc. 29851 Willow Creek Road Eugene, OR 97402-9132 Phone (541) 465-8300 Fax (541) 335-0504</small>		<small>Printed Apr 12, 2018</small>	

MOLECULAR PROBES®		CERTIFICATE OF ANALYSIS	
<b>Catalog Number</b>	F8811	<b>Catalog Number</b>	F8811
<b>Product Name</b>	FluoSpheres® carboxylate-modified microspheres, 0.2 $\mu\text{m}$ , yellow-green fluorescent (505/515) *2% solids*	<b>Product Name</b>	FluoSpheres® carboxylate-modified microspheres, 0.2 $\mu\text{m}$ , yellow-green fluorescent (505/515) *2% solids*
<b>Appearance</b>	yellow suspension	<b>Appearance</b>	yellow suspension
<b>Medium</b>	distilled water, 2 mM azide	<b>Medium</b>	distilled water, 2 mM azide
<b>Concentration</b>	$5.3 \times 10^{12}$ particles/mL	<b>Concentration</b>	$5.3 \times 10^{12}$ particles/mL
<b>Lot Number</b>	1927586	<b>Lot Number</b>	1927586
SONICATE WELL BEFORE USE. STORE AT 2° - 8° C, DO NOT FREEZE			
	LOT DATA	SPECIFICATION	
<b>FLUORESCENCE</b>			
Emission Maximum <sup>1</sup>	513 nm		515 $\pm$ 5 nm
Relative Quantum Yield <sup>2</sup>	0.19		$\geq$ 0.15
<b>MICROSCOPY</b>			
Inspection	meets specification		few or no aggregates detectable after sonication
<b>TECHNICAL DATA<sup>3</sup></b>			
Actual Particle Size	$0.19 \pm 0.0140 \mu\text{m}$		n.a.
Charge	0.872 meq/g		n.a.
Density of Polystyrene	1.055 g/cm <sup>3</sup>		n.a.
Specific Surface Area	$3.0 \times 10^5 \text{ cm}^2/\text{g}$		n.a.
<b>MISCELLANEOUS INFORMATION</b>			
Material Lot Number	1919822		n.a.
<ol style="list-style-type: none"> <li>Excitation: 490 nm.</li> <li>Relative to a solution in methanol of the dye used to prepare this product.</li> <li>Technical data for the unstained microspheres.</li> </ol>			
 Rachel Smith, Quality Assurance Manager 20-Sep-2017			
<small>Life Technologies Corporation, on behalf of its Invitrogen business, Molecular Probes® labeling and detection technologies, certifies on the date above that this is an accurate record of the analysis of the subject lot and that the data conform to the specifications in effect for this product at the time of analysis.</small>			
<small>Molecular Probes, Inc. 29851 Willow Creek Road Eugene, OR 97402-9132 Phone (541) 465-8300 Fax (541) 335-0504</small>		<small>Printed Nov 22, 2017</small>	

Supplementary Figure 1.1: Certificates of Analysis for a) FS<sub>100</sub> and b) FS<sub>200</sub>, showing values for charge density of each material.

## 2. Binding Ratio Determination

**Supplementary Table 2.1:** Concentration ranges used for binding experiments on all nanoparticles.

Nanoparticle	[NP] tested	[BSA] tested	[BSA]:[Nanoparticle] ratio range
FS <sub>100</sub>	0.5 – 1 nM	400 – 5000 nM	200 – 10 000
FS <sub>200</sub>	0.0625 – 1 nM	200 – 5000 nM	200 – 80 000
QD	1 nM	100 – 1600 nM	5 – 80
DOTAP	1 nM	30 – 1200 nM	30 – 1000

### 2.1. FS<sub>100</sub> and FS<sub>200</sub> binding ratios

#### 2.1.1. Product Formation model

An equilibrium expression is shown in Equation 2.1, where P represents one BSA protein, S represents one FS, and n represents an integer of free proteins which bind to the FS over time. This equilibrium assumes that only one type of protein-FS complex is being formed in solution, which simplifies the reality of the distribution. Consequently, we assume that the single FS-BSA complex represents the average BSA to FS binding ratio.



BSA bound to a FS surface likely exhibits an occupancy distribution in reality, however to simplify our calculations we presume an average number of BSA proteins per sphere and one type of complex in solution. We can then assume that both the brightness of BSA ( $\eta_p$ ) and the FS ( $\eta_s$ ) do not change upon protein-NP binding, which leads to the following association:

$$\eta_{bp} = n\eta_{fp} \quad \text{Eq. 2.2}$$

Where the subscripts *bp* and *fp* represent bound and free protein, respectively. Cross-correlation amplitudes are proportional to the number of complexes in solution (Experimental Methods, Equation 1.4). Assuming that all FS are occupied with proteins at equilibrium, and using Equations 2.1 and 2.2,  $G_x(0)$  can be described as the following:

$$G_x(0) = \frac{n\eta_{fp}\eta_s N_s}{(\eta_{fp}N_{fp} + n\eta_{fp}N_{bp})(\eta_s N_{is})} \quad \text{Eq. 2.3}$$

Where  $N$  is the number of emitters in the TPE volume. Using Equation 2.3, theoretical cross-correlation amplitude values were calculated from hypothetical binding ratios using known values for protein and FS concentration and brightness at initial conditions and at equilibrium. These amplitudes were plotted against binding ratio and used as a “standard curve” to extrapolate binding ratio using experimental amplitudes (Supplementary Figure 2.1a).

#### 2.1.1 Free Protein Reduction model

An autocorrelation amplitude depends on the brightness of the fluorescent entity,  $\eta_i$ , and the number of unique fluorescence emitters,  $N_i$ , in the focal volume summed over all unique emitters,  $i$ , as described in Equation 2.4, which is an extension of Experimental Methods Equation 1.2.

$$G(0) = \frac{\sum_i \eta_i^2 N_i}{(\sum_i \eta_i N_i)^2} \quad \text{Eq. 2.4}$$

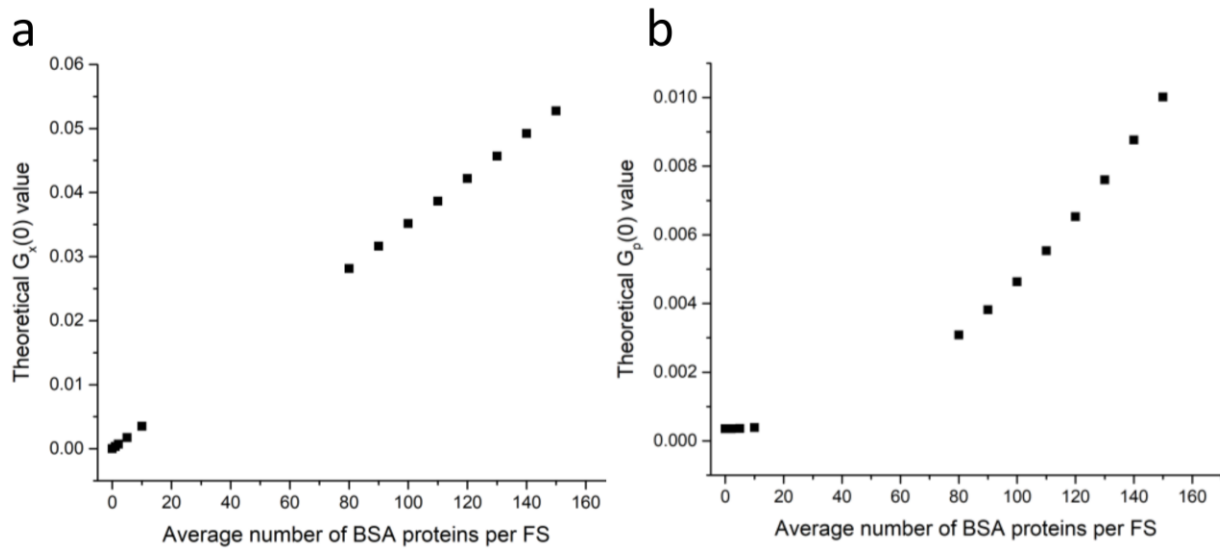
Applying this to the case of the protein data, we can presume that BSA is either free, or an  $n$  number are bound to the FS. From Equation 2.4, the quantities of protein can be measured using autocorrelation analysis, and this can be expanded to specify free and bound proteins as shown in Equation 2.5:

$$G_p(0) = \frac{\eta_{fp}^2 N_{fp} + \eta_{bp}^2 N_{bp}}{(\eta_{fp} N_{fp} + \eta_{bp} N_{bp})^2} \quad \text{Eq. 2.5}$$

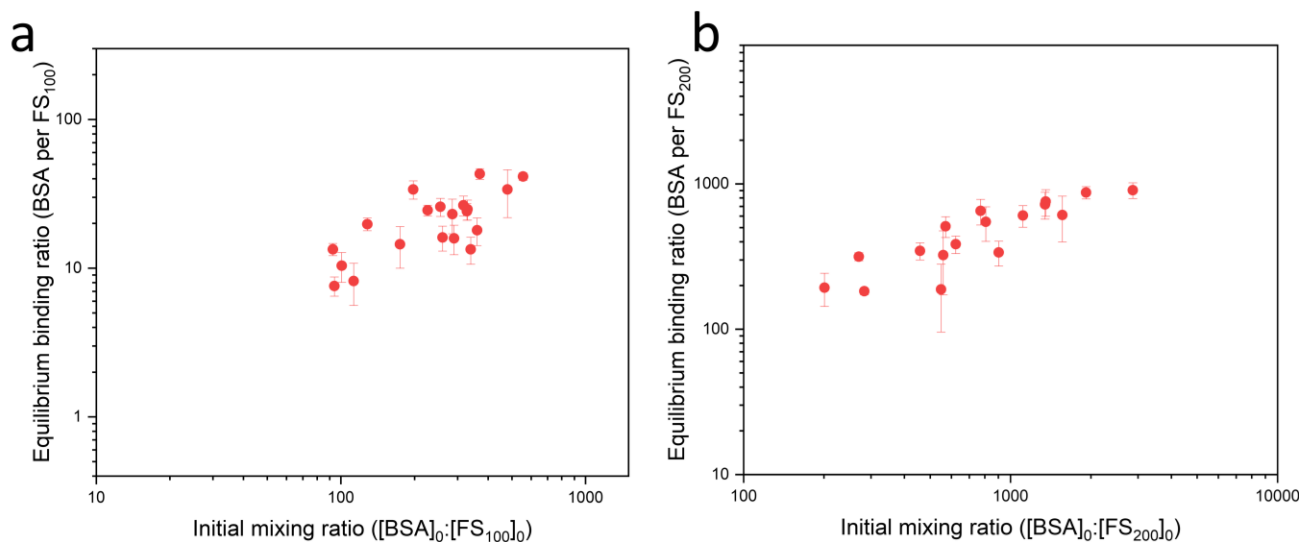
This further allows, through substitution of Equation 2.5 into Equation 2.4, a simple  $G_p(0)$  expression for the protein that relates initial concentrations and experimental  $G_p(0)$  amplitudes to equilibrium binding ratios:

$$G_p(0) = \frac{N_{fp} + n^2 N_{bp}}{(N_{fp} + n N_{bp})^2} \quad \text{Eq. 2.6}$$

Theoretical amplitude values were calculated from hypothetical binding ratios using known values for protein  $N$  at initial conditions and at equilibrium. These amplitudes were plotted against binding ratio and used as a “standard curve” to extrapolate binding ratio using experimental amplitudes (Supplementary Figure 2.1b). Binding plots from  $G_p(0)$  data are given in Supplementary Figure 2.2 and show similar maximum binding ratios to those calculated from  $G_x(0)$ .



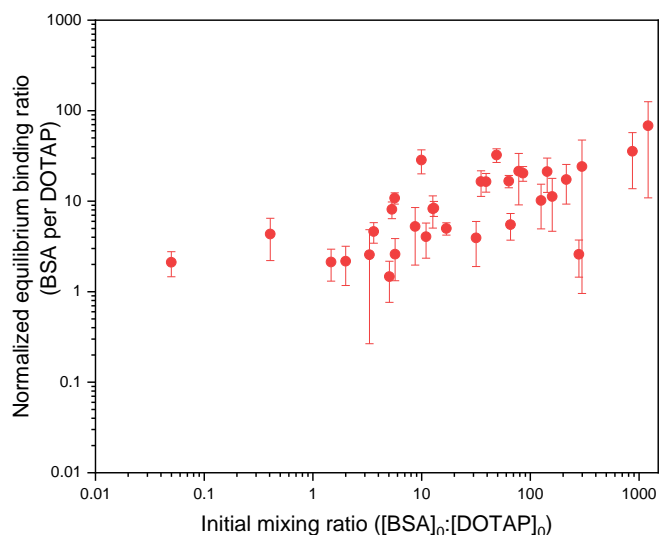
**Supplementary Figure 2.1:** Example resulting **a)**  $G_x(0)$  and **b)**  $G_p(0)$  values calculated from hypothetical binding ratios, using Equations 2.3 and 2.5, respectively.



**Supplementary Figure 2.2:** Average number of BSA proteins on FS surfaces at dynamic equilibrium calculated from  $G_p(0)$  data, as a function of initial mixing ratio of protein to nanoparticle. Data shown are for **A)** FS<sub>100</sub>, **B)** FS<sub>200</sub>. Error bars represent standard deviation of technical replicates (n=3) propagated through binding ratio calculations.

### 2.2. DOTAP binding ratios

Binding ratios were determined using the same methods as for the FS systems. Binding ratios are normalized to liposome diameter by multiplying by a correction factor relating measured hydrodynamic diameter to a 200 nm diameter standard, to account for batch variation in liposome preparation. Binding plots from  $G_p(0)$  data are given in Supplementary Figure 2.3 and show similar maximum binding ratios to those calculated from  $G_x(0)$ .



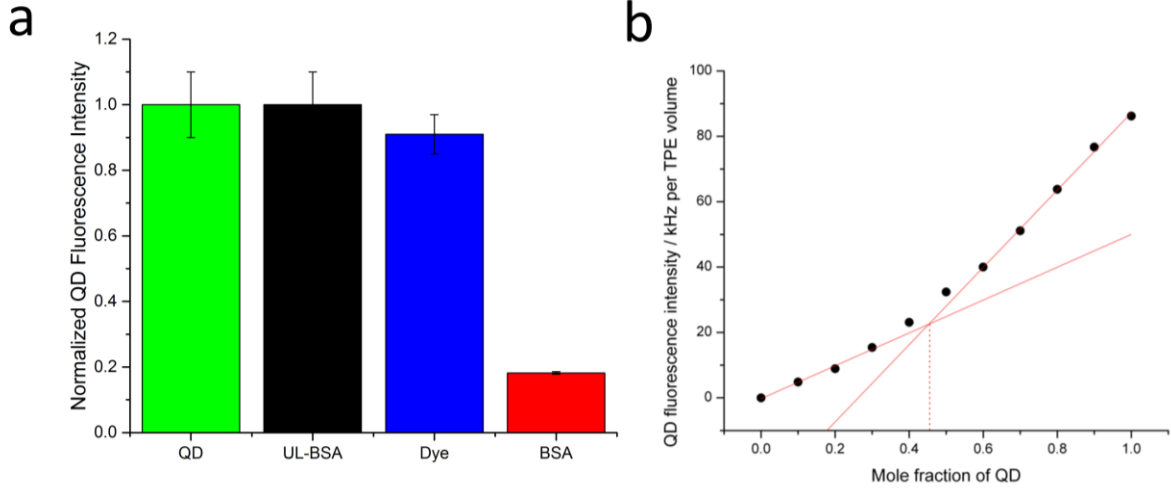
**Supplementary Figure 2.3:** Average number of BSA proteins on DOTAP calculated from  $G_p(0)$  data at dynamic equilibrium, as a function of initial mixing ratio. Data is normalized to a liposome diameter of 200 nm to account for batch variation between preparations. Error bars represent standard deviation of technical replicates (n=3) propagated through binding ratio calculations.

### 2.3. QD binding ratios

QD-BSA FRET was established to occur as a result of protein-NP binding based on control experiments where fluorescence of QD alone was compared to QD in the presence of unlabeled BSA, labeled BSA, and labeling dye alone (Supplementary Figure 2.4a). This established as well that binding was not driven by the dye as FRET was only observed when the dye was attached to a protein. Using the method of continuous variation, a plot was created that correlated the fluorescence intensity of the quantum dots to the mole fraction of the quantum dots in the QD-BSA mixture to determine the equilibrium binding ratio under low-protein

conditions (Supplementary Figure 2.4b). Because of this energy transfer, at other protein concentrations, it was possible to calculate the binding ratio using FRET efficiency (Equation 2.7).  $F_{DA}$  is fluorescence intensity of a FRET donor with a receptor and  $F_D$  is the fluorescence intensity of the same donor without a receptor present.  $R_0$  is the Förster radius and  $r$  is the donor-acceptor distance.

$$n = \frac{F_D - F_{DA}}{F_{DA}} \left(\frac{r}{R_0}\right)^6 \quad \text{Eq. 2.7}$$



**Supplementary Figure 2.4 a)** Bar graph of 20 nM QD (green) fluorescence intensity, with the addition of 800 nM unlabeled BSA (black), 1600 nM dye (blue), or 800 nM labeled BSA (red). The errors represent the standard deviation obtained from triplicates. **b)** Job's plot of the QD-BSA interactions to determine the binding ratio between QD and BSA. The binding ratio between BSA and QDs is determined from the x- coordinate of the point of intersection from the two red tangent lines. A mole fraction of 0.46 for the quantum dots translates to a BSA to QD binding ratio of 1.2:1.

### 3. Equilibrium constants

#### 3.1. DOTAP, FS<sub>100</sub>, and FS<sub>200</sub> equilibrium constants

The association constant,  $K_A$ , (plotted in main text, Figure 3) was defined in terms of the concentration of occupied and available receptor sites on the NP ( $[bound\ sites]$  and  $[free\ sites]$ , respectively) and the concentration of free protein in solution ( $[P_{free}]$ ) after the establishment of an equilibrium.

$$K_A = \frac{[bound\ sites]}{[P_{free}][free\ sites]} \quad \text{Eq. 3.1}$$

The concentration of free NP sites available for binding was determined using the following:

$$[free\ sites] = \left[ \frac{n_{max} - \frac{n}{NP}}{TPE\ volume} \right] \quad \text{Eq. 3.2}$$

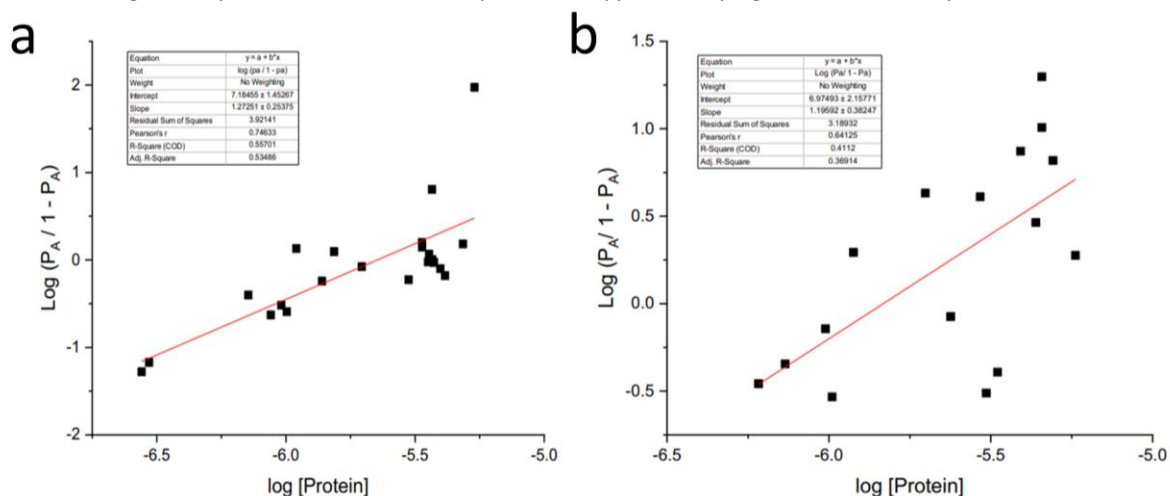
The concentration of occupied NP sites at equilibrium was determined by using the following:

$$[bound\ sites] = \left[ \frac{\frac{n}{NP}}{TPE\ volume} \right] \quad \text{Eq. 3.3}$$

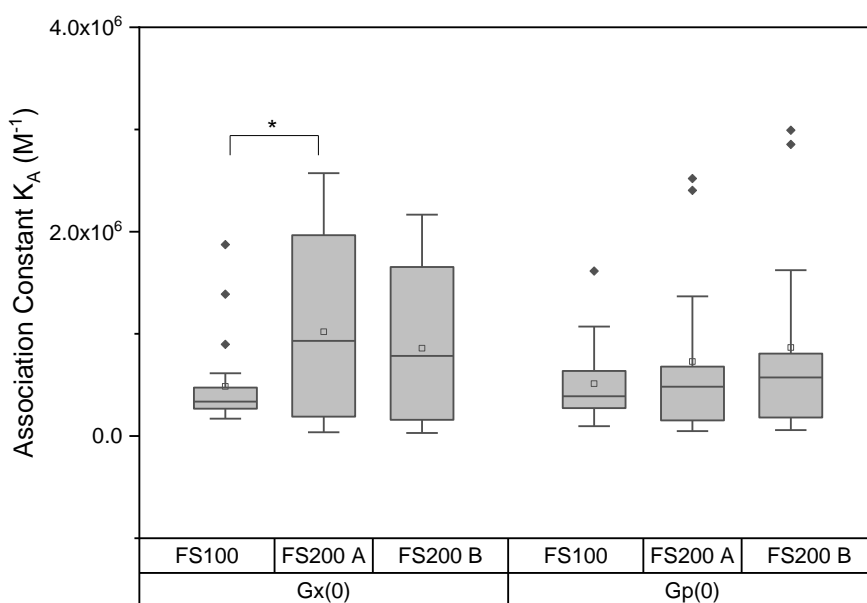
The concentration of free protein in solution upon reaching the equilibrium binding was determined by taking the difference in the total initial amount of protein available  $[P_{tot}]$  minus the protein bound to NP at equilibrium, which could be found by multiplying the equilibrium binding ratio by the concentration of NP in solution,  $[NP]$ .

$$[P_{free}] = [P_{tot}] - \left(\frac{n}{NP} \cdot [NP]\right) \quad \text{Eq. 3.4}$$

In the FS<sub>100</sub> case, the slope of the linearized hill plot is approximately 1.3 and suggests little to no cooperativity in binding (Supplementary Figure 3.1a). Similarly, for the FS<sub>200</sub> system, the Hill coefficient is approximately 1.2 (Supplementary Figure 3.1b). Surface area and charge density normalized K<sub>A</sub> values are plotted in Supplementary Figure 3.2 for the FS systems.



**Supplementary Figure 3.1:** Linearized Hill plots for the equilibrated systems composed of the **a)** red-labeled FS<sub>100</sub> (1 nM) and green-labeled BSA and **b)** yellow-green-labeled FS<sub>200</sub> (1 nM) and red-labeled BSA. Slope is indicated in the “m” row of each results table. Red lines show the linear fits described by the parameter boxes.



**Supplementary Figure 3.2:** Association constants for the different sized FS in both the G<sub>x</sub>(0)-derived K<sub>A</sub> values and the G<sub>p</sub>(0)-derived K<sub>A</sub> values. FS<sub>200A</sub> represents data normalized to the surface area of FS<sub>100</sub> particles, whereas FS<sub>200B</sub> represents data normalized to the surface charge density of the FS<sub>100</sub> particles. Significance shown as \* (p < 0.05) calculated using two-sample t-tests.

### 3.2. QD equilibrium constants

Because the experimental results from the QD binding were more complex than the FS systems, the number of proteins per QD was not directly accessible from FCCS. Nevertheless, at equilibrium between free and protein-saturated QDs, the QD-protein binding can be described by:



where Q represents QDs, P represents proteins,  $QP_n$  represents the QD-protein complex, and n is the binding ratio between QDs and proteins. In a simple model where  $n = 1$ , the concentration of the 1:1 complex ( $[QP]$ ) can be calculated from the association constant ( $K=[QP]/([Q][P])$ ), the initial QD concentration ( $[Q]_0$ ), and the initial protein concentration ( $[P]_0$ ), as shown in Equation 3.6.

$$[QP] = \frac{(K([Q]_0 + [P]_0) + 1) - \sqrt{(K([Q]_0 + [P]_0) + 1)^2 - 4K^2[Q]_0[P]_0}}{2K} \quad \text{Eq. 3.6}$$

If the brightness of the free and bound QDs is  $\eta_0$  and  $\eta_1$ , respectively, the QD average fluorescence intensity ( $\langle F \rangle$ ) can be calculated using Equation 3.7.

$$\langle F \rangle = \eta_0[Q]_0 + (\eta_1 - \eta_0)[QP] \quad \text{Eq. 3.7}$$

Combining Equations 3.6 and 3.7 gives Equation 3.8, allowing K to be accessed from  $\langle F \rangle$ ,  $\eta_i$ ,  $[Q]_0$ , and  $[P]_0$ .

$$\langle F \rangle = \eta_0[Q]_0 + (\eta_1 - \eta_0) \frac{(K([Q]_0 + [P]_0) + 1) - \sqrt{(K([Q]_0 + [P]_0) + 1)^2 - 4K^2[Q]_0[P]_0}}{2K} \quad \text{Eq. 3.8}$$

In addition, the  $G(0)$  value for QDs can be calculated using Equation 3.9.

$$G(0) = \frac{\eta_0^2[Q] + \eta_1^2[QP]}{(\eta_0[Q] + \eta_1[QP])^2 \cdot V \cdot N_A} \quad \text{Eq. 3.9}$$

In a more complicated system that consists of both 1:1 ( $QP$ ) and 1:2 ( $QP_2$ ) complexes, the two QD-protein binding steps can be described by the following equations, where  $K_{A1}$  and  $K_{A2}$  are the association constants for the first and second protein adsorption, respectively.



$$K_{A1} = \frac{[QP]}{[Q][P]} \quad \text{Eq. 3.12}$$

$$K_{A2} = \frac{[QP_2]}{[QP][P]} \quad \text{Eq. 3.13}$$

The concentration of the free QDs ( $[Q]$ ) can be described using Equation 3.14 below.

$$[Q] = [Q]_0 - [QP] - [QP_2] = [Q]_0 - K_1[Q][P] - K_1K_2[Q][P]^2 = \frac{[Q]_0}{1 + K_1[P] + K_1K_2[P]^2} \quad \text{Eq. 3.14}$$

The QD average fluorescence intensity can then be calculated using Equation 3.15

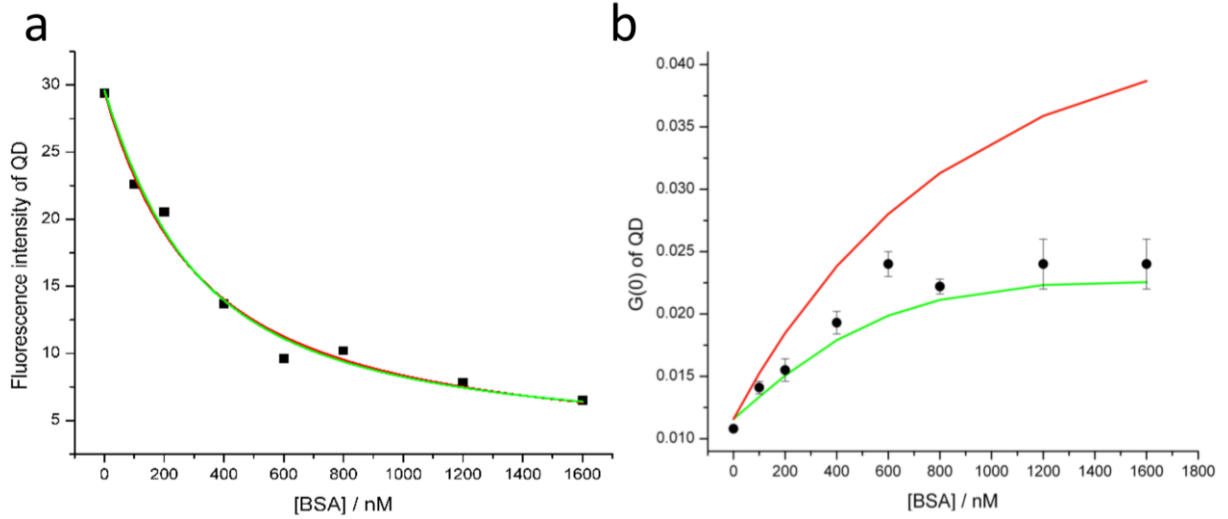
$$\begin{aligned} \langle F \rangle &= \eta_0[Q] + \eta_1[QP] + \eta_2[QP_2] \\ \langle F \rangle &= \frac{[Q]_0(\eta_0 + \eta_1K_1[P] + \eta_2K_1K_2[P]^2)}{1 + K_1[P] + K_1K_2[P]^2} \end{aligned} \quad \text{Eq. 3.15}$$

The QD  $G(0)$  values can be calculated using Equation 3.16 below.

$$G(0) = \frac{\eta_0^2[Q] + \eta_1^2[QP] + \eta_2^2[QP_2]}{(\eta_0[Q] + \eta_1[QP] + \eta_2[QP_2])^2}$$

$$G(0) = \frac{(1 + K_1[P] + K_1K_2[P]^2)(\eta_0^2 + \eta_1^2K_1[P] + \eta_2^2K_1K_2[P]^2)}{[Q]_0(\eta_0 + \eta_1K_1[P] + \eta_2K_1K_2[P]^2)^2 \cdot V \cdot N_A} \quad \text{Eq. 3.16}$$

Parameters of  $\eta_1$ , and  $K_A$  were recovered from the fittings in Supplementary Figure 3.3a. The recovered parameters were used to calculate the  $G(0)$ s for QDs using Equation 3.9 for a 1:1 ratio case and Equation 3.16 for the case involving both 1:1 and 1:2 complexes. The calculated and experimental values for the  $G(0)$  were compared to check the reliability of the results obtained from the QD fluorescence fittings. As shown in Supplementary Figure 3.3b, the experimental  $G(0)$  values do not agree with those calculated assuming simple 1:1 binding behavior. The  $G(0)$  values (green curve in Supplementary Figure 3.3b calculated using the assumption of both types of complex agree well with the measured data (black squares in Supplementary Figure 3.3b) which confirms that our system contains a mixture of 1:1 and 1:2 QD:BSA complexes at the concentration regimes tested. Because of the nature of the data used to access  $K_A$  values, rather than a different  $K_A$  retrieved for each BSA:QD ratio as seen for the FS and DOTAP systems, one  $K_A$  was obtained for each of the two first steps in early binding.



**Supplementary Figure 3.3:** **a)** Decrease in QD average fluorescence intensity with BSA concentration. The red curve shows the fitting with Equation 2.16 based on the simpler scenario. The green curve shows the fitting with Equation 2.23 considering both 1:1 and 1:2 complexes. **b)** Comparison of the measured (black squares) and predicted (red curve calculated assuming 1:1 complex; green curve calculated assuming a mixture of 1:1 and 1:2 complexes) QD  $G(0)$  values. The error bars in the experimental data correspond to the standard deviations of independent measurements. The residuals for the two comparisons are shown in the bottom panel (red circles: calculated assuming 1:1 complex; green triangles: calculated assuming a mixture of 1:1 and 1:2 complexes).

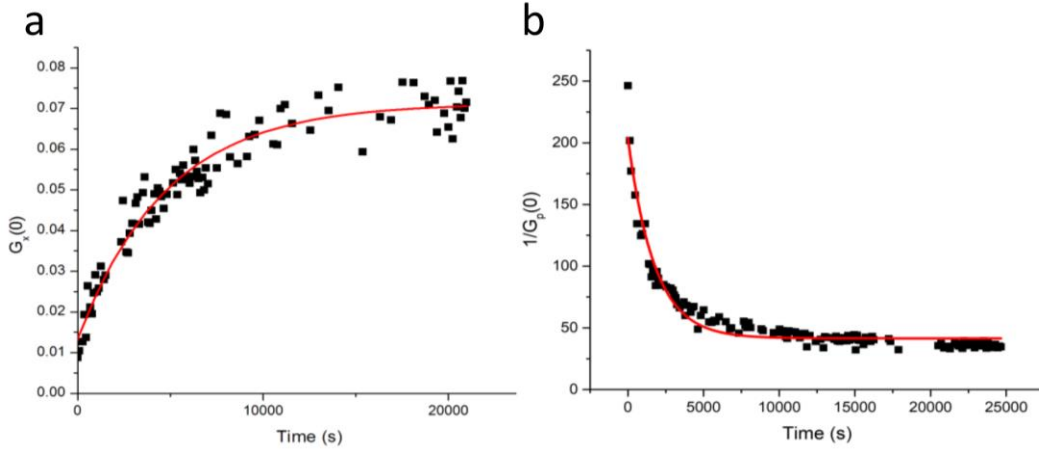
#### 4. Kinetics Data

##### 4.1. FS<sub>100</sub>, FS<sub>200</sub>, and DOTAP

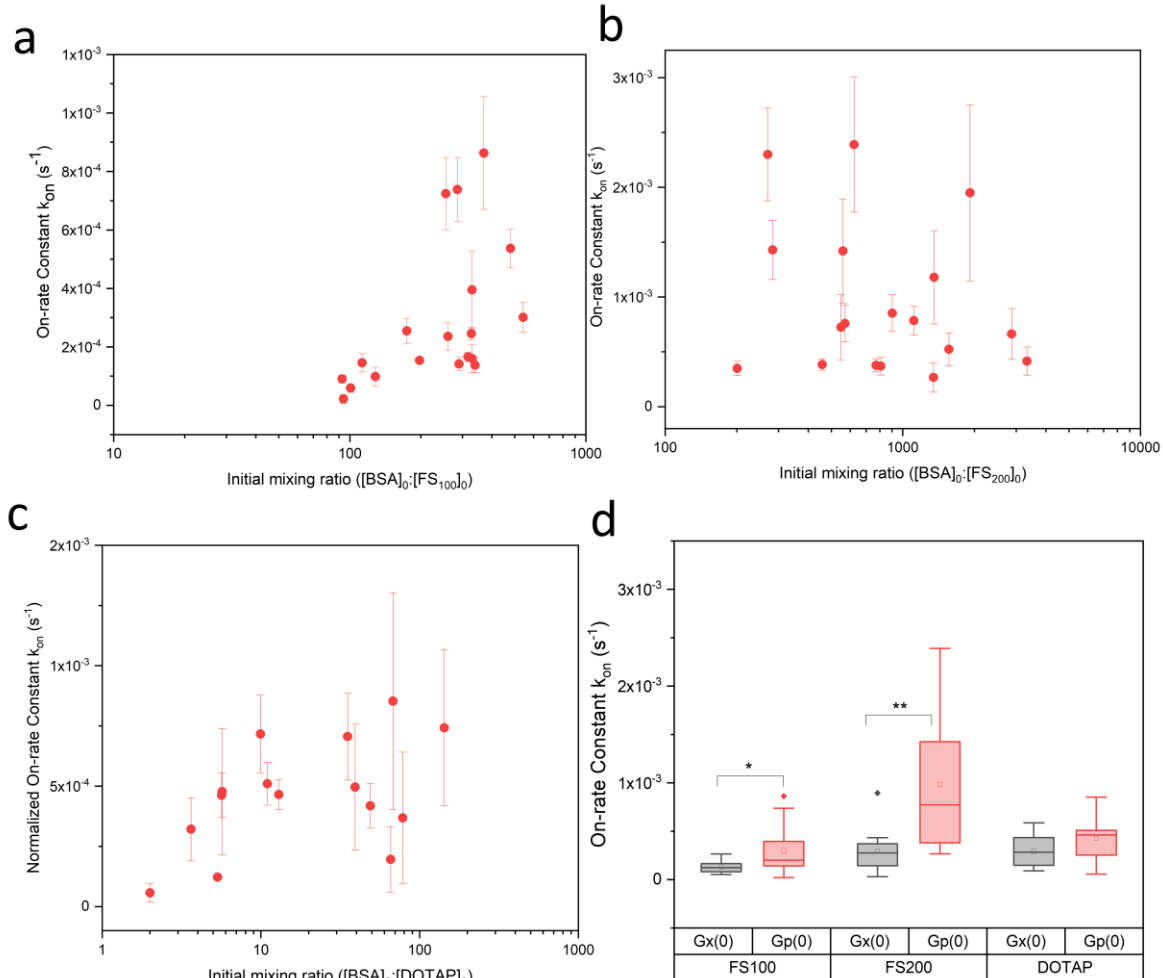
For FS<sub>100</sub>, FS<sub>200</sub>, and DOTAP,  $G_x(0)$  values were plotted over experimental time and fitted to with Equation 2.24 to calculate a rate constant,  $k_{on}$  (Supplementary Figure 4.1a). For both the FS and DOTAP systems, changes in apparent protein concentration (from FCS analysis) as a function of time could be fitted to with an exponential decay function to determine an on-rate in addition to retrieving this value by monitoring complex formation. This was done by plotting  $1/G_p(0)$  as a function of time and fitting with Equation 2.25 to calculate  $k_{on}$  (Supplementary Figure 4.1b). No evidence of FRET was observed for these systems.

$$G_x(t) = G_x(0)_{equilib}(1 - e^{-k_{on}t}) + G_x(0)_{t=0} \quad \text{Eq. 4.1}$$

$$G_p(0)^{-1}(t) = G_p(0)^{-1}_{t=0} e^{-k_{on}t} + G_p(0)^{-1}_{equilib} \quad \text{Eq. 4.2}$$



**Supplementary Figure 4.1:** Example plots of **a)** cross-correlation amplitudes, and **b)** inverse of autocorrelation amplitudes, versus time, for the FS systems. Mono-exponential fits (shown in red) were chosen for simplicity, but bi-exponential behavior may exist in these data sets. The red lines represent fits to the data using equations 2.8 and 2.9 for panels (a) and (b), respectively.



**Supplementary Figure 4.2:** On-rate constants obtained from  $G_p(0)$  data for mixtures of NPs with BSA as a function of initial protein:NP ratio. Data shown are for **a)** FS<sub>100</sub>, **b)** FS<sub>200</sub>, and **c)** DOTAP. DOTAP data is normalized to a liposome diameter of 200 nm to account for slight batch variation between liposome preparations. Panel **d)** shows significant differences between the kinetic on-rate constants for the particles from the  $G_x(0)$ -derived and the  $G_p(0)$  data, calculated using two-sample t-tests. Significance shown as \* ( $p < 0.05$ ) and \*\* ( $p < 0.01$ ). Error bars correspond to propagation of triplicate standard deviation errors through the calculations

The provided  $G_p(0)$  results are included here (Supplementary Figure 4.2a-c) as a confirmation of the binding we are observing through  $G_x(0)$  analysis. The former protein-based method yielded larger  $k_{on}$  values for all systems than the complex-formation method (Supplementary Figure 4.2d) but after further analysis, it was determined that this method was convoluted by many factors. Firstly, autocorrelation amplitude reports not only on reduction of freely diffusing protein, but on protein that is complexed to NPs as well. Further, correlator hardware exclusively detects changes in fluorescence, and may detect many proteins bound to a NP surface as a single protein, with an increased brightness and diffusion coefficient equivalent to that of the NP. Although the complex-formation data is also convoluted by the distribution of species within solution, the formulae used to analyze this data is influenced less by this physical complexity than formulae used in analyzing autocorrelation data. Because of this, it was determined that  $k_{on}$  derived by the evolution of complex formation exclusively is a more accurate depiction of kinetics.

**Supplementary Table 3.1:** Kinetic on-rates, off-rates, and residence times for BSA onto FS and DOTAP NPs. Errors represent SEM over  $n$  biological replicates.

NP	On-Rate Constant ( $s^{-1}$ )	Off-Rate Constant ( $s^{-1}$ )	Approx. Residence Time (s)	n
FS <sub>100</sub>	$(1.3 \pm 0.1) \times 10^{-4}$	$(1.2 \pm 0.6) \times 10^{-1}$	8	19
FS <sub>200</sub>	$(2.9 \pm 0.5) \times 10^{-4}$	$(2.5 \pm 2.0) \times 10^{-2}$	39	15
DOTAP	$(2.9 \pm 0.4) \times 10^{-4}$	$(2.0 \pm 1.8) \times 10^{-2}$	50	18

#### 4.2. QD Kinetics Data

We know from the FRET data and equilibrium binding ratios that the brightness of the QD species in solution displays the following order  $\eta_{QD} > \eta_{QD:BSA} > \eta_{QD:BSA_2}$  and that at low mixing ratios (less than 10), the end product is largely a single BSA associated with each QD (QD:BSA). At higher mixing ratios, higher order complexes are formed. Therefore, binding equations can be written:



Thus, the differential rate laws become the following:

$$\frac{d[QD]}{dt} = -k_1[QD][BSA] \quad \text{Eq. 4.5a}$$

$$\frac{d[QD:BSA]}{dt} = k_1[QD][BSA] - k_2[QD:BSA][BSA] + k_{-2}[QD:BSA_2] \quad \text{Eq. 4.5b}$$

$$\frac{d[QD:BSA_2]}{dt} = k_2[QD:BSA][BSA] - k_{-2}[QD:BSA_2] \quad \text{Eq. 4.5c}$$

We consider that most of the experiments performed were at excess of BSA. Therefore, the on-rate constants in Equations 4.5a and 4.5b contain a linear dependence on  $[BSA]$  ( $k_{on}' = k_{on} * [BSA]$ ). From this, Equations 4.5 (a-c) can be simplified:

$$\frac{d[QD]}{dt} = -k_1'[QD] \quad \text{Eq. 4.6a}$$

$$\frac{d[QD:BSA]}{dt} = k_1'[QD] - k_2'[QD:BSA] + k_{-2}[QD:BSA_2] \quad \text{Eq. 4.6b}$$

This allows for analytic solutions of the differential rate equations given the following integrated rate equations:

$$[QD] = [QD]_0 e^{-k'_1 t} \quad \text{Eq. 4.7a}$$

$$[QD : BSA] = [QD]_0 \left( \frac{k_{-2}}{k'_2 + k_{-2}} + \frac{k_{-2} + k'_1}{k'_1 - k'_2 - k_{-2}} e^{-k'_1 t} + \frac{k'_1 k'_2}{(k'_2 + k_{-2})(k'_1 - k'_2 - k_{-2})} e^{-(k'_2 + k_{-2})t} \right) \quad \text{Eq. 4.7b}$$

$$[QD : BSA_2] = [QD]_0 \left( \frac{k'_2}{k'_2 + k_{-2}} + \frac{k'_2}{k'_1 - k'_2 - k_{-2}} e^{-k'_1 t} + \frac{-k'_1 k'_2}{(k'_2 + k_{-2})(k'_1 - k'_2 - k_{-2})} e^{-(k'_2 + k_{-2})t} \right) \quad \text{Eq. 4.7c}$$

The total luminescence is the sum of the luminescence from all components. We propose that the shape of the luminescence vs. time plot can be modelled as a natural outcome of the relative brightness of the various QD components and a simple two step mechanism. In main text Figure 6a the luminescence decays are fitted to using the following equation:

$$I_{fl}(t) = \eta_{QD}[QD](t) + \eta_{QD:BSA}[QD : BSA](t) + \eta_{QD:BSA_2}[QD : BSA_2](t) \quad \text{Eq. 4.8}$$

where the time dependent concentrations evolve according to the integrated rate laws derived above. For ratios 5 and 10, the fits use only the first integrated rate equation since at equilibrium there is only a single BSA associated with the QD. Assuming a pseudo first-order reaction based on how the recovered rate constant from the fitting ( $k_{on1}^{obs}$ ) depended on protein concentration for the ratios where only binding of one BSA occurs, the true first on-rate constants ( $k_1$ ) were calculated using Equation 2.16 below:

$$k_1 = \frac{k_1^{obs}}{[BSA]_0 + \frac{1}{K_{eq}}} \quad \text{Eq. 4.9}$$

Where  $K_{eq}$  is for the first step of binding (see SI 3.2).

## 5. Statistical Analysis

**Supplementary Table 4.1:** Statistical values for Welch's two-sample t-tests to compare means, assuming unequal variance in all comparisons due to different numbers of replicates.

Figure	Comparison	T statistic	Degrees Freedom	P value
Main Figure 3d	FS <sub>100</sub> vs FS <sub>200</sub> K <sub>A</sub>	-4.09156	14.31217	0.00105
	FS <sub>100</sub> vs FS <sub>200</sub> k <sub>on</sub>	-3.04288	15.5592	0.00795
Main Figure 4d	FS <sub>200</sub> vs DOTAP k <sub>on</sub>	0.03131	25.84348	0.97527
	FS <sub>100</sub> vs DOTAP k <sub>on</sub>	-4.20509	20.88613	4.01882E-4
Supplementary Figure 2.6	FS <sub>100</sub> vs FS <sub>200A</sub> K <sub>A</sub>	-2.25735	19.00884	0.03595
	G <sub>x</sub> (0) data	FS <sub>100</sub> vs FS <sub>200B</sub> K <sub>A</sub>	-1.81852	20.98856
Supplementary Figure 2.6	FS <sub>100</sub> vs FS <sub>200A</sub> K <sub>A</sub>	-0.87349	15.04486	0.39612
	G <sub>p</sub> (0) data	FS <sub>100</sub> vs FS <sub>200B</sub> K <sub>A</sub>	-1.21797	14.15558
Supplementary Figure 2.9d	FS <sub>100</sub> G <sub>x</sub> (0) vs G <sub>p</sub> (0) k <sub>on</sub>	-2.79212	18.48175	0.01183
	FS <sub>200</sub> G <sub>x</sub> (0) vs G <sub>p</sub> (0) k <sub>on</sub>	-3.69211	17.54358	0.00173
	DOTAP G <sub>x</sub> (0) vs G <sub>p</sub> (0) k <sub>on</sub>	-1.95536	27.21276	0.06088

## 6. Supplementary References

- (1) Swift, J. L.; Heuff, R.; Cramb, D. T. A Two-Photon Excitation Fluorescence Cross-Correlation Assay for a Model Ligand-Receptor Binding System Using Quantum Dots. *Biophys. J.* **2006**, *90* (4), 1396–1410. <https://doi.org/10.1529/biophysj.105.069526>.
- (2) Nguyen, T. T.; Swift, J. L.; Burger, M. C.; Cramb, D. T. Effects of Various Small-Molecule Anesthetics on Vesicle Fusion: A Study Using Two-Photon Fluorescence Cross-Correlation Spectroscopy. *J. Phys. Chem. B* **2009**, *113* (30), 10357–10366. <https://doi.org/10.1021/jp901089k>.
- (3) Zhang, H. Thin-Film Hydration Followed by Extrusion Method for Liposome Preparation; Humana Press, New York, NY, 2017; pp 17–22. [https://doi.org/10.1007/978-1-4939-6591-5\\_2](https://doi.org/10.1007/978-1-4939-6591-5_2).
- (4) Huang, B. X.; Kim, H.-Y.; Dass, C. Probing Three-Dimensional Structure of Bovine Serum Albumin by Chemical Cross-Linking and Mass Spectrometry. *J Am Soc Mass Spectrom* **2004**, *15*, 1237–1247. <https://doi.org/10.1016/j.jasms.2004.05.004>.
- (5) Bacia, K.; Schwille, P. Practical Guidelines for Dual-Color Fluorescence Cross-Correlation Spectroscopy. *Nat. Protoc.* **2007**, *2* (11), 2842–2856. <https://doi.org/10.1038/nprot.2007.410>.